Cell

CRIg: A Macrophage Complement Receptor Required for Phagocytosis of Circulating Pathogens

Karim Y. Helmy,[1,5] Kenneth J. Katschke, Jr.,[1,5] Nick N. Gorgani,[1] Noelyn M. Kljavin,[2] J. Michael Elliott,[3] Lauri Diehl,[4] Suzie J. Scales,[2] Nico Ghilardi,[2] and Menno van Lookeren Campagne[1,*]
[1] Department of Immunology, Genentech Inc., 1 DNA Way, South San Francisco, CA 94080, USA
[2] Department of Molecular Biology, Genentech Inc., 1 DNA Way, South San Francisco, CA 94080, USA
[3] Department of Protein Chemistry, Genentech Inc., 1 DNA Way, South San Francisco, CA 94080, USA
[4] Department of Pathology, Genentech Inc., 1 DNA Way, South San Francisco, CA 94080, USA
[5] These authors contributed equally to this work.
*Contact: menno@gene.com
DOI 10.1016/j.cell.2005.12.039

SUMMARY

The complement system serves an important role in clearance of pathogens, immune complexes, and apoptotic cells present in the circulation. Complement fragments deposited on the particle surface serve as targets for complement receptors present on phagocytic cells. Although Kupffer cells, the liver resident macrophages, play a dominant role in clearing particles in circulation, complement receptors involved in this process have yet to be identified. Here we report the identification and characterization of a Complement Receptor of the Immunoglobulin superfamily, CRIg, that binds complement fragments C3b and iC3b. CRIg expression on Kupffer cells is required for efficient binding and phagocytosis of complement C3-opsonized particles. In turn, Kupffer cells from CRIg-deficient mice are unable to efficiently clear C3-opsonized pathogens in the circulation, resulting in increased infection and mortality of the host. CRIg therefore represents a dominant component of the phagocytic system responsible for rapid clearance of C3-opsonized particles from the circulation.

INTRODUCTION

The liver plays a dominant role in the clearance of particles from the bloodstream through Kupffer cells (KCs), which represent the major phagocytic constituent of the reticuloendothelial system (Benacerraf et al., 1959). KCs are strategically positioned in liver sinusoids to efficiently phagocytose pathogens from portal and arterial blood, preventing infection of various organs. Phagocytosis of circulating pathogens by tissue resident macrophages is primarily dependent on the presence of Fc receptors (reviewed by Ravetch and Bolland, 2001) and receptors for complement components (Brown, 1991). In the absence of antibodies, complement serves as the dominant opsonin contributing to pathogen clearance by phagocytes. Complement component C3 is central to the activation of all three complement pathways: the alternative, classical, and mannose binding lectin pathways (reviewed by Walport, 2001a, 2001b). C3 binds to bacterial surfaces via a thioester bond after cleavage to C3b, a subunit of active C3 convertase. This step catalyzes the cleavage of additional C3 molecules that then serves as a multivalent ligand for complement receptors (CRs) expressed on phagocytic cells (Pangburn and Muller-Eberhard, 1980). Mice and humans lacking C3 are highly susceptible to bacterial and viral infections (reviewed by Colten and Rosen, 1992), demonstrating the central importance of C3 in the innate immune defense.

Four complement C3 fragment receptors, CR1 (CD35), CR2 (CD21), CR3 (CD11b/CD18), and CR4 (CD11c/CD18), have been described to date (reviewed by Holers et al., 1992). In the mouse, CR1/2 is expressed on B cells and follicular dendritic cells (Fang et al., 1998) and CR4 on dendritic cells (Metlay et al., 1990), but none of these receptors have been described as functional complement receptors on KCs. Low levels of CR3 are expressed on KCs but do not appear to be involved in the rapid hepatic clearance of complement C3-opsonized pathogens (Gregory et al., 2002; Wu et al., 2003). Thus, the putative receptor on KCs critical for complement-mediated clearance of circulating pathogens has so far not been described.

Here we report the identification of a novel complement receptor, CRIg, which is uniquely expressed on tissue resident and sinusoidal macrophages and whose structure and function are conserved in humans and mice. In contrast to known complement receptors described to date, CRIg is found on a constitutively recycling pool of

membrane vesicles and participates in the internalization of C3-opsonized particles from the circulation by KCs. Mice lacking CRIg are unable to efficiently clear pathogens in the circulation, demonstrating that CRIg is a critical component of the innate immune system.

RESULTS

CRIg Is Expressed on a Subset of Tissue Resident Macrophages

CRIg was cloned as part of the Secreted Protein Discovery Initiative (SPDI; Clark et al., 2003) in search for homologs of the junctional adhesion molecule (JAM) family. CRIg is a type 1 transmembrane Ig superfamily member and exists as two alternatively spliced forms. The longer form of human CRIg, huCRIg(L), encodes both V and C_2-type terminal Ig domains (Smith and Xue, 1997; Figure S1A), while the short form, huCRIg(S), encodes a single V-type Ig domain. Murine CRIg (muCRIg) encodes only one form with a single IgV-type domain (Figures 1A and S1A). huCRIg(L) is also known as Z39Ig, a molecule first described by Langnaese et al., (2000). Z39Ig mRNA is expressed in human monocytes differentiated with M-CSF and IL4 (Ahn et al., 2002) and in cDNA libraries from human synovium, lung, and placenta (Walker, 2002). The cytoplasmic domains of human and murine CRIg contain consensus AP-2 internalization motifs, YARL and DSQALI, respectively (Bonifacino and Traub, 2003). HuCRIg(S) and muCRIg share 67% overall sequence homology, with 83% homology residing in the IgV domain. CRIg is most closely related to A33 antigen and JAM-A, although sequence similarity is confined to a conserved stretch of residues forming the Ig domain fold (results not shown). Both human and murine CRIg are located on the X chromosome at position Xq12 between *hephaestin* and *moesin*.

Consistent with the two alternatively spliced forms of human CRIg, Northern blot analysis revealed a 1.7 kB transcript and a lesser expressed 1.4 kB transcript. The highest levels of human transcripts were detected in the placenta, lung, adrenal gland, heart, and liver, with lower levels in the other organs. A single transcript of ~1.4 kB was detected in mouse liver and heart (Figure S1B).

Monoclonal antibodies were generated against human and murine CRIg to define the expression of CRIg protein. Human and murine CRIg were absent on peripheral blood $CD19^+/B220^+$ B-cells, $CD3^+$ T cells, $CD56^+/NK1.1^+$ NK cells, and $CD15^+/Ly6G^+$ granulocytes (Figure S1). huCRIg was absent on peripheral blood $CD14^+$ monocytes but was readily detected on monocyte-derived macrophages (MDMs) by flow cytometry (Figure 1B). Similar to huCRIg, muCRIg was absent on $F4/80^+$ peripheral blood monocytes but was detected on $F4/80^+$ liver KCs (Figure 1B) and a subset of resident peritoneal macrophages (Figure 1C and results not shown). Expression of huCRIg(L) and (S) protein was confirmed as 50 and 45 K Mr proteins on monocytes differentiated into macrophages (Figure 1C). Similarly, muCRIg was detected as a 45 K Mr glycoprotein in peritoneal macophages (PM). muCRIg has a predicted N-linked glycosylation site, and its glycosylation accounts for a −5 kDa mobility shift shown by SDS gel-electrophoresis (results not shown).

We further analyzed CRIg expression in the liver by immunohistochemistry. CRIg was expressed on $CD68^+$ KCs in human and mouse liver (Figure 1D) and interstitial macrophages in the heart (results not shown). In humans, CRIg was also detected in adrenal gland macrophages, alveolar macrophages, Hofbauer cells, synovial macrophages, and lamina propria histiocytes (results not shown). CRIg was absent from human and mouse splenic macrophages, Langerhans cells, microglial cells, and bone-marrow-derived macrophages as well as from a variety of human and mouse monocyte/macrophage cell lines (THP-1, RAW264.7, PU5-1.8, P388D1, WEHI-3, J774, and IC-21; results not shown). Together, these results indicate that CRIg is highly expressed on liver KCs as well as on subsets of macrophages resident in various tissues.

CRIg Binds C3b and iC3b

The expression of CRIg on a population of highly phagocytic cells prompted us to explore whether CRIg was involved in binding of opsonized particles. Complement and Fc receptors have been demonstrated to mediate phagocytosis of serum-opsonized particles (reviewed by Aderem and Underhill, 1999; Underhill and Ozinsky, 2002). To determine whether CRIg binds to complement C3 fragments deposited on a cell surface, sheep erythrocytes coated with rat IgM (E-IgM) were incubated with Jurkat T cells stably transfected with huCRIg(L) in the presence or absence of C3. CRIg(L)-expressing Jurkat cells, but not empty vector-transfected cells, formed rosettes with E-IgM in the presence (C3+), though not absence (C3−), of C3 (Figure 2A). CRIg did not appear to be involved in Fc-receptor-mediated binding since sheep erythrocytes opsonized with only IgG did not rosette with Jurkat-CRIg cells (results not shown).

To test whether CRIg can directly bind complement components on cell surfaces, a soluble form of human CRIg was generated in which the extracellular domain of CRIg was fused to the Fc portion of human IgG1. huCRIg(L)-Fc, but not control-Fc, fusion protein bound to E-IgM opsonized in C3-deficient serum that was reconstituted with increasing concentrations of purified human C3 (Figure 2B). Both huCRIg(S)-Fc and muCRIg-Fc were capable of binding to E-IgM, indicating that the V-type Ig domain was sufficient for this interaction (results not shown).

During complement activation and particle opsonization, C3 is cleaved into its multiple breakdown products, each of which could serve as a binding partner for CRIg. By ELISA, huCRIg(L)- and huCRIg(S)-Fc, but not control-Fc, demonstrated saturable binding to C3b, iC3b (Figure 2C), and methylated C3 (results not shown) but not to C3, C3a, or C3d (results not shown). Similar binding specificity was observed for extracellular domain of CRIg lacking the Fc portion and for muCRIg-Fc (results not shown). No binding activity was detected with C1, C2,

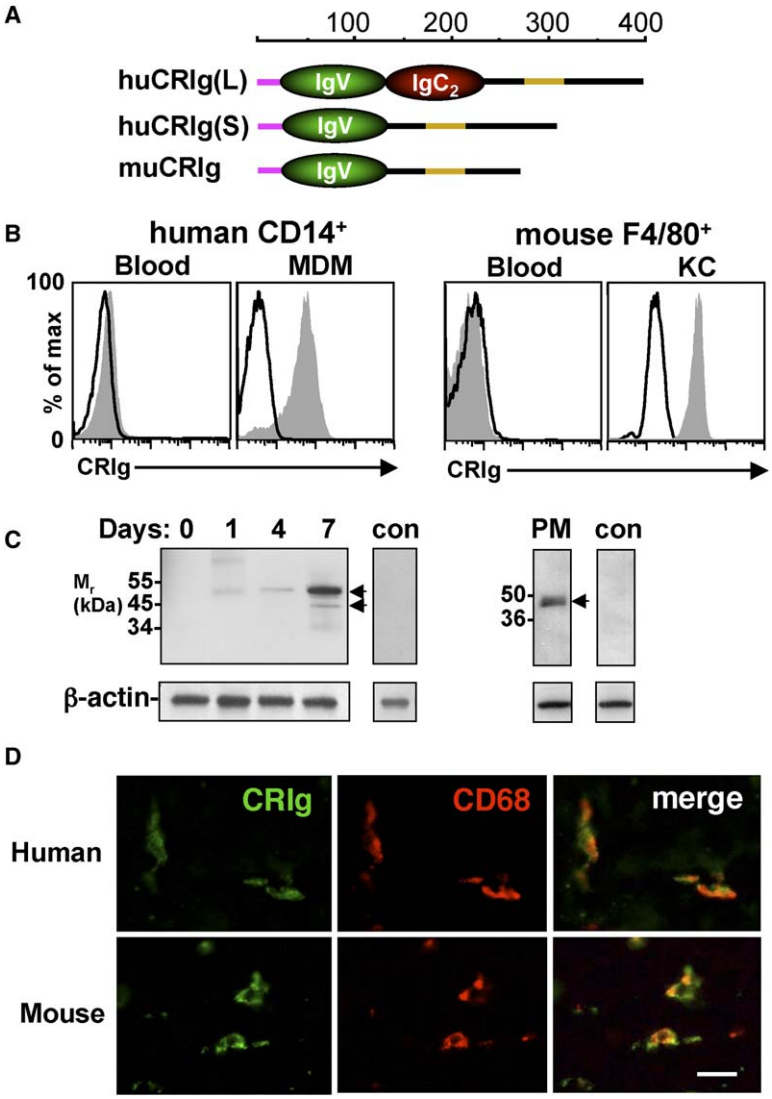

Figure 1. CRIg Is Selectively Expressed on a Subpopulation of Tissue Resident Macrophages

(A) CRIg is a single transmembrane immunoglobulin superfamily member consisting of either an IgV and IgC_2-type domain (huCRIg(L)) or one IgV-type immunoglobulin domain (huCRIg(S) and muCRIg). The signal sequence and transmembrane domain are indicated in purple and yellow. The scale indicates size in amino acids.

(B) CRIg is expressed in macrophages but not in monocytes. Human $CD14^+$ monocytes and 7-day monocyte-derived macrophages (MDM) were analyzed for huCRIg staining by flow cytometry using anti-huCRIg mAb (clone 3C9; left panels, shaded histograms). Mouse $F4/80^+$ peripheral blood monocytes and liver KCs were analyzed for muCRIg staining using an anti-muCRIg mAb (clone 14G6; right panels, shaded histograms). Open histograms: isotype-matched controls.

(C) Western blot analysis of whole-cell lysates from human MDMs cultured up to 7 days and of mouse peritoneal macrophages. Western blots were incubated with a polyclonal anti-CRIg antibody (left panels) or an anti-muCRIg monoclonal antibody (right panels). Preimmune rabbit IgG and rat IgG2b were used as isotype-matched controls (con). Arrows in the left panel indicate the position of 50 and 45 K Mr proteins; arrow in right panel indicates the position of muCRIg protein (45 K Mr). Anti-β actin was used to demonstrate equal loading.

(D) Colocalization of CRIg with CD68 on liver KCs. Immunostaining was performed on sections obtained from human or mouse liver using monoclonal anti-CRIg (green channel) and anti-CD68 (red channel) antibodies. The yellow color in the merged panels indicates colocalization. Scale bar = 10 μm.

C4, C4b, C5, C6, and C9 (results not shown). Conversely, soluble C3b also bound to plate-coated huCRIg(L)-Fc and was competed off by huCRIg(L)-ECD (results not shown). Hence, CRIg can bind C3b and iC3b both in solution and when bound to a substrate. Because C3b is present in multimeric form when deposited on particle surfaces (Hong et al., 1991) or immunoglobulins (Jelezarova et al., 2003), we further assessed the binding of huCRIg(L) to C3b dimers ($C3b_2$, Arnaout et al., 1981). $C3b_2$ bound to huCRIg(L)-Fc with a Kd of 131 nM (results not shown) and to huCRIg(S)-Fc with a Kd of 44 nM, as measured by surface plasmon resonance (Figure 2D).

To complement these biochemical studies, we evaluated the binding specificity of cell-surface CRIg for C3-derived products. A488-labeled $C3b_2$ bound to the surface of CRIg(L)-expressing THP-1 cells (Figure 2E). This binding was competed off by the addition of soluble unlabeled $C3b_2$, C3b monomer, and huCRIg(L)-ECD, though not by native C3. In addition to binding to soluble complement fragments, muCRIg expressed on the surface of CHO cells also bound to various particles opsonized in C3-sufficient serum (Figure S2). Together, our studies demonstrate that both soluble and cell-surface-expressed CRIg bind C3b and iC3b protein and opsonized particles.

CRIg Is Required for Binding of C3 Fragments to Kupffer Cells

To study its physiological function, mice lacking CRIg were generated by homologous recombination (Figure S3A). Deletion was confirmed by Southern blotting of genomic DNA (Figure S3B), Western blotting of peritoneal macrophage cell lysates, and flow cytometry of KCs (Figure 3A). CRIg knockout (ko) mice were born at the expected Mendelian ratios and exhibited no gross phenotypic or histopathological abnormalities. Absolute numbers of immune cells in different lymphoid compartments were similar in blood (Figure S3C), spleen, and lymph nodes (results not shown) from wild-type (wt) and ko animals. In addition,

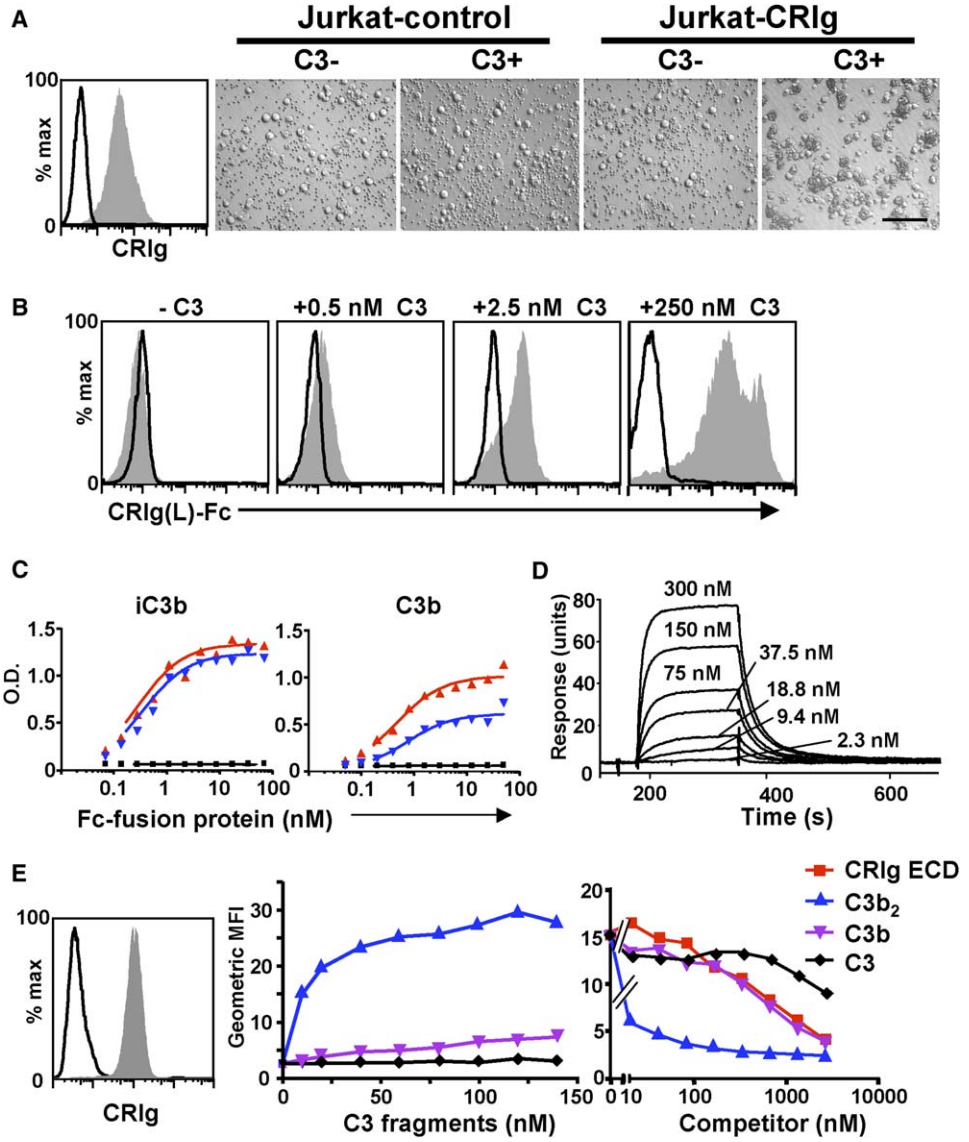

Figure 2. Cell Surface-Expressed and Soluble CRIg Bind to C3 Fragments

(A) huCRIg(L)-transfected Jurkat cells (Jurkat-CRIg, shaded histogram), but not empty vector-transfected Jurkat cells (Jurkat-control, open histogram), form rosettes with E-IgM incubated with C5-depleted (C3+), though not C3-depleted (C3−), serum. Results shown are representative of three independent experiments. Scale bar = 100 μm.

(B) huCRIg(L)-Fc binding to E-IgM is C3 dependent. E-IgM, opsonized with C3-depleted human serum to which increasing concentrations of purified human C3 were added, were incubated with a huCRIg(L)-Fc fusion protein and an anti-human Fc polyclonal antibody for flow cytometry detection. Results shown are representative of three independent experiments.

(C) Binding of huCRIg(L)- and huCRIg(S)-Fc to C3b and iC3b. Increasing concentrations of huCRIg(L)-Fc (red symbols) and huCRIg(S)-Fc- (blue symbols) or control Fc- (black symbols) fusion proteins were added to maxisorp plates coated with purified C3b or iC3b. Binding was detected using an HRP-conjugated anti-huFc antibody and expressed in Optical Densities (O.D.) of the converted TMB substrate. Results shown are representative of four independent experiments using different batches of fusion protein and purified complement components.

(D) Kinetic binding data showing soluble C3b dimers ($C3b_2$) binding to huCRIg(S)-Fc. The affinity of $C3b_2$ for the CRIg fusion proteins was determined using surface plasmon resonance. CRIg fusion proteins were captured on a CM5 sensor chip using an antibody directed to the Fc fusion tag. $C3b_2$ was injected for 180 s. The Kd was calculated from binding curves showing response at equilibrium plotted against the concentration. $C3b_2$ bound to huCRIg(S) with a calculated affinity of 44 nM and to huCRIg(L) with 131 nM affinity.

(E) $C3b_2$, though not native C3, binds to cell surface-expressed CRIg. Left panel: histogram showing CRIg expression on huCRIg(L)-transfected (shaded histogram), though not empty vector-transfected (open histogram), THP-1 cells by flow cytometry. Middle panel: flow cytometry analysis of binding of A488 conjugated C3b, $C3b_2$, and C3 to huCRIg(L)-transfected THP-1 cells following incubation for 30 min at 4°C. Right panel: $C3b_2$ binding to THP-1 CRIg was competed off by $C3b_2$, to a lesser extent by C3b and the extracellular domain of huCRIg(L) (CRIg ECD), and by C3 only at higher concentrations. Results shown are representative of three independent experiments.

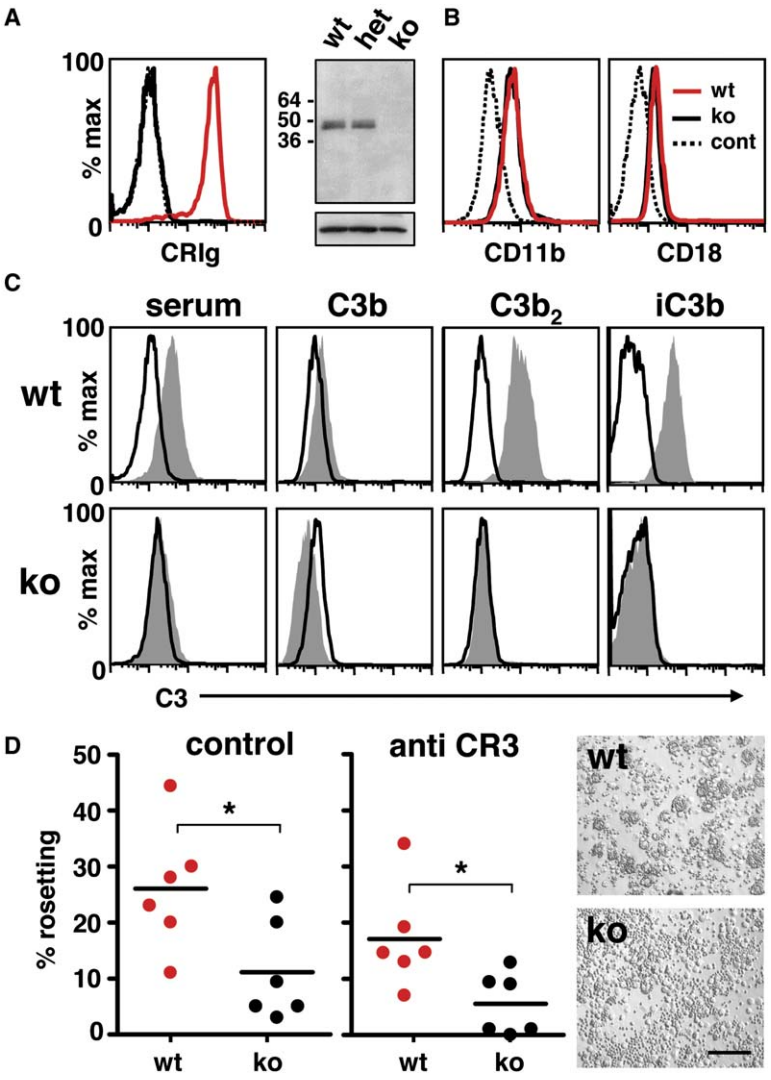

Figure 3. Expression of CRIg on Kupffer Cells Is Required for Binding of C3b and iC3b

(A) CRIg protein is absent on macrophages obtained from CRIg ko mice. Left panel: Kupffer Cells (KCs) from CRIg wt (red line) and ko mice (black solid line) were incubated with A488 conjugated 14G6 or an isotype control antibody (dotted line) and analyzed by flow cytometry. KCs were gated as indicated in Figure S3D. Right panel: peritoneal macrophages obtained from CRIg wt, het, or ko mice were lysed and Western blotted with an anti-muCRIg mAb (14G6) using anti-β-actin as a loading control.

(B) KCs isolated from CRIg wt or ko mice express similar levels of complement receptor CR3. KCs isolated from livers of CRIg wt and ko mice were stained with antibody to F4/80, CD11b, CD18 and, an isotype control (cont) and analyzed by flow cytometry.

(C) CRIg is required for binding to C3 fragments. KCs isolated from CRIg wt or ko mice were incubated with activated mouse serum (activated by incubation for 30 min at 37°C) or purified C3b, $C3b_2$, iC3b, and PE-conjugated anti-F4/80. Binding of C3 components to KCs was detected by incubation with a polyclonal anti-mouse or-human C3 antibody recognizing the various C3-derived fragments (shaded histograms). Control samples (open histograms) were incubated with secondary antibody only. Results shown are representative of four experiments.

(D) KCs isolated from CRIg ko mice show decreased rosetting to mouse serum-opsonized E-IgM. KCs isolated from livers of CRIg wt and ko mice were incubated with E-IgM opsonized with C3-sufficient mouse serum for 30 min at 37°C in the presence of isotype-matched control antibody or anti-CR3 blocking antibody (clone M1/70, 25 μg/ml). Cells were fixed, and the number of KCs that formed rosettes with E-IgM were counted and expressed as a percentage of the total number of KCs. * = $p < 0.05$, Student's t test. Results shown are representative of two independent experiments. Images on the right depict E-IgM rosettes on CRIg wt and ko KCs in the presence of control antibody. Scale bar = 50 μm.

no differences were observed in the number of $F4/80^+$ KCs or heart macrophages when analyzed by flow cytometry and immunohistochemistry, respectively (results not shown). Expression levels of other complement binding proteins on KCs, including the α and β chains of CR3 (CD11b and CD18), were not altered (Figure 3B). In addition, expression of complement receptor 1-related protein y (Crry) and the low or undetectable expression of CR1, CR2, or CD11c, the α chain of CR4, were similar between wt and ko KCs (Figure S4A).

To analyze the binding capacity of CRIg wt and CRIg ko KCs to C3 degradation products, C3 fragments were generated by incubation of serum at 37°C. C3 fragments in the activated serum as well as purified $C3b_2$ and iC3b readily bound to the surface of CRIg wt KCs, whereas no C3 degradation fragments were bound to CRIg ko KCs (Figure 3C). Minimal binding of C3b monomer (Figure 3C) and no binding of C3 to either wt or ko KCs were detected (Figure S4B). To extend our analysis from the binding of soluble C3 fragments to the binding of C3 fragments bound to particle surfaces, we examined the requirement for CRIg on KCs to bind mouse serum-opsonized E-IgM. CRIg ko KCs demonstrated a −60% reduction in E-IgM rosetting when compared to CRIg wt KCs (Figure 3D). CR3 had a minor contribution to total binding activity, as a further reduction (−20%) in rosette formation was

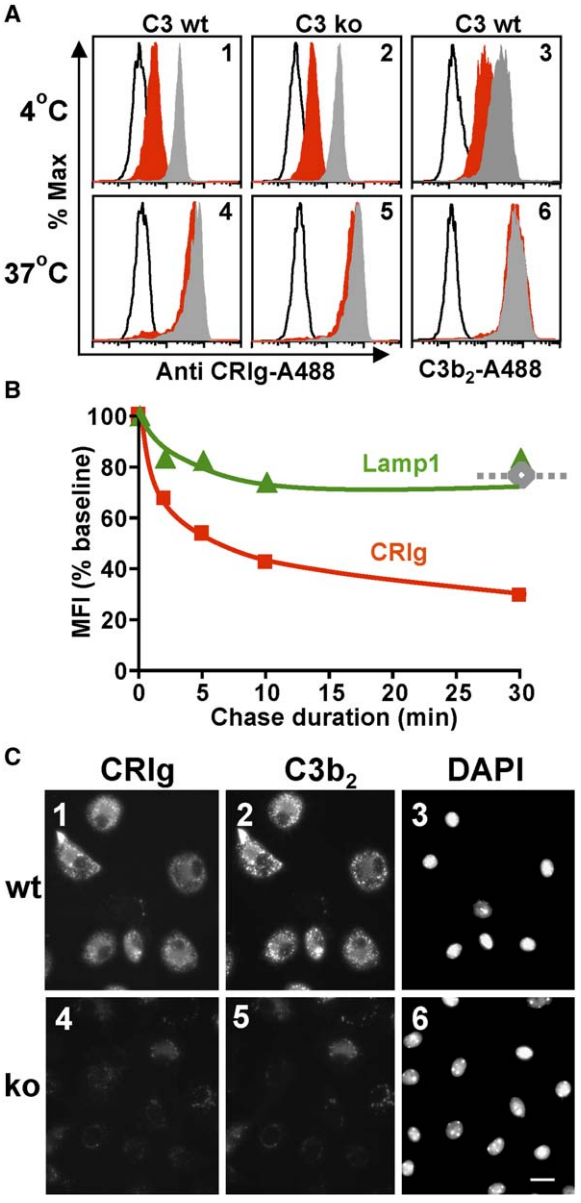

Figure 4. CRIg on Kupffer Cells Recycles

(A) CRIg internalizes independently of ligand binding. KCs from C3 wt (panels 1, 3, 4, and 6) or C3 ko mice (panels 2 and 5) were incubated with A488-conjugated anti-CRIg antibody 14G6 or $C3b_2$ for 1 hr at 4°C (panels 1–3) or for 10 min at 37°C (panels 4–6). Cells were returned to 4°C and incubated with (solid red) or without (solid gray) quenching anti-A488 antibody to distinguish cytoplasmic from cell surface bound anti-CRIg antibodies or $C3b_2$. Open histograms show KCs incubated with isotype-matched control antibody.

(B) CRIg, but not Lamp1, antibodies recycle to the cell surface. KCs pooled from two mice were loaded with A488-conjugated anti-muCRIg or anti-muLamp1 antibodies for 10 min at 37°C, washed, and subsequently incubated for indicated time periods at 37°C in the presence of anti-A488 quenching antibodies. Mean fluorescence intensity (MFI) was monitored by flow cytometry as a function of time. Indicated are the mean of two independent experiments. The gray symbol and dotted line indicate fluorescence from anti-muCRIg antibodies in the absence of quenching antibodies.

observed with the addition of a CR3-blocking antibody. Hence, CRIg expression is necessary for binding of C3 degradation products and C3-opsonized particles to KCs.

CRIg Internalizes and Is Localized on Recycling Endosomes

As binding of C3-opsonized particles to its receptors may trigger their subsequent internalization (Fearon et al., 1981; Sengelov et al., 1994), we applied a surface quenching technique (Austin et al., 2004) to investigate whether CRIg and C3b are internalized into KCs. A488-conjugated anti-CRIg mAbs were preincubated with KCs at 4°C. Addition of anti-A488 antibodies at 4°C quenched most fluorescence from surface-bound A488-conjugated anti-CRIg antibodies (Figure 4A, panel 1). When A488-conjugated anti-CRIg mAbs were incubated with KCs at 37°C for 15 min followed by incubation with anti-A488 antibodies on ice, fluorescence was not quenched (Figure 4A, panel 4), indicating that the anti-CRIg antibodies had internalized during the 37°C incubation and were no longer accessible to quenching antibodies. Similar results were found for the internalization of $C3b_2$ (Figure 4A, panels 3 and 6). Internalization of anti-CRIg antibodies was not dependent on the presence of C3 since uptake of the antibody occurred similarly in KCs isolated from C3 ko mice (Figure 4A, panels 2 and 5). When KCs preloaded with A488-conjugated anti-CRIg antibodies were incubated at 37°C in the presence, though not in the absence, of extracellular quenching antibodies, a decrease in fluorescence over time was observed, suggesting that anti-CRIg antibodies recycle back to the cell surface (Figure 4B). The time course of recycling was again independent of C3, as the kinetics of quenching was similar in the presence or absence of C3 (results not shown). In contrast, A488-conjugated antibodies to the lysosomal protein Lamp1 were internalized but did not appreciably recycle, remaining mostly unquenched with time. Immunofluorescent microscopy further confirmed the colocalization of anti-CRIg antibodies and $C3b_2$ on cytoplasmic vesicles in KCs from CRIg wt, but not ko, mice (Figure 4C). These results indicate that CRIg functions as a receptor for C3b and is located on a pool of constitutively recycling membranes.

To further determine the subcellular compartments in which CRIg recycles, huMDMs were visualized by epifluorescence microscopy using transferrin as a marker for recycling endosomes and Lamp1 as a marker for lysosomes. MDMs cultured for 7 to 12 days express CRIg on ~50% of the cells and demonstrate saturable binding of C3b, but not of C4b (Figure S5A), that can be competed off with the extracellular domain of huCRIg(L)

(C) Internalization and colocalization of CRIg and $C3b_2$ in CRIg wt, but not CRIg ko, KCs. KCs isolated from the livers of CRIg wt and ko mice were cultured in chamber slides for 2 days and incubated with A555-conjugated anti-CRIg (14G6) antibodies and A488-conjugated $C3b_2$ for 30 min at 37°C, mounted in DAPI containing mounting medium, and photographed. Scale bar = 10 μm.

(results not shown). Macrophages labeled with anti-CRIg antibody at 4°C (to prevent internalization) demonstrate focal CRIg expression in F-actin rich filopodial extensions (arrowheads in Figure 5A). In addition, the CRIg antibody colocalized with C3b on the cell surface (results not shown). Transfer of cells from 4°C to 37°C for 10 min resulted in rapid internalization of CRIg antibody and C3b into transferrin$^+$ endosomes located in the periphery of the cell (Figure 5B, arrows), clearly distinct from the more perinuclear Lamp1$^+$ lysosomal compartment (Figure S5C, arrows). CRIg remained almost completely colocalized within the transferrin compartment and was not significantly accumulated in lysosomes in the presence of lysosomal protease inhibitors even after prolonged chase times of up to 24 hr (results not shown). Internalized CRIg antibodies completely overlapped with the total steady-state pool of CRIg detected postfixation with a polyclonal antibody, indicating that the addition of anti-CRIg antibodies did not influence CRIg recycling (Figure S5D, panels 1–3). CRIg trafficking was independent of the presence of C3 in the medium (Figure S5D, panel 4). Together, these results further support the conclusion that CRIg is present on recycling and early endosomes and that CRIg internalizes and recycles constitutively independently of C3-derived ligand or anti-CRIg antibodies.

Since the majority of in vivo C3b and iC3b is deposited on particles (Brown, 1991), we next explored the distribution of CRIg in macrophages during phagocytosis of C3-opsonized particles. Upon encounter with C3 containing serum-opsonized E-IgM, CRIg rapidly (within 10 min) redistributed from transferrin-positive vesicles to the phagocytic cups (arrowhead in Figure 5C) and phagosomes (arrows in Figures 5C and S5E) forming around the engulfed erythrocytes. This redistribution was absent when the E-IgM were opsonized in C3-depleted human serum (results not shown). During this initial stage of phagocytosis, CRIg$^+$ phagosomes were located in the periphery of the cell, away from the perinuclear Lamp1$^+$ lysosomal compartment (Figure 5C, arrows), and were devoid of transferrin, suggesting active sorting of CRIg to the forming phagosome membrane. After incubation for 2 hr, these phagosomes had matured, as determined by the colocalization of the E-IgM with the Lamp1$^+$ lysosomal compartment (Figure 5D, arrowheads). Whereas CRIg continued to be expressed on the earlier phagosomal membranes surrounding some of the C3-opsonized E-IgM (Figure 5D, thin arrows), most of the Lamp1$^+$ phagosomes lacked CRIg. The complete absence of CRIg from the Lamp1$^+$ membranes was unlikely the result of lysosomal degradation of CRIg because lysosomal protease inhibitors were continuously present during the incubation. Furthermore, in macrophages containing only mature (Lamp1$^+$) phagosomes, CRIg colocalized with the transferrin$^+$ compartment (Figure 5D, thick arrows), suggesting that CRIg returns to the recycling compartment prior to (or during) fusion of the E-IgM-containing phagosome with the lysosomal compartment.

Taken together, these results indicate that CRIg is actively recruited from recycling endosomes to sites of C3b-coated particle ingestion and participates in the initial stages of phagosome formation. CRIg then recycles from the phagosome prior to phagosome-lysosome fusion to return to the endosomal compartment, thus avoiding degradation.

CRIg Is Required for Clearance of C3-Opsonized Pathogens

Based on the binding of CRIg to C3b/iC3b-opsonized particles, we set out to explore a role for CRIg in the innate response of mice to intravenously injected, complement-opsonized bacteria. *Listeria monocytogenes* (LM) is an intracellular pathogen whose major route of infection is through the gastrointestinal tract (reviewed by Vazquez-Boland et al., 2001; Portnoy et al., 2002; Dussurget et al., 2004). In the present study, LM was injected intravenously to study the role of CRIg in removal of the pathogen from the blood. In line with a role for CRIg in phagocytosis of C3-opsonized particles, CRIg ko KCs had internalized significantly fewer bacteria compared to CRIg wt KCs (Figure 6A). As a result, the number of live bacteria recovered in the liver of CRIg ko mice was significantly lower (by 9.7 million CFUs) than in CRIg wt mice, and the sum of the bacterial counts in blood, spleen, and lung was significantly higher (in total by 9.5 million colony-forming units (CFUs) in CRIg ko compared to CRIg wt mice (Figure 6B). Clearance of circulating bacteria by the liver was also compromised in CRIg wt mice treated with a CRIg-Fc fusion protein (Figure S6A) and in CRIg wt mice treated with a CRIg-iC3b-blocking antibody (results not shown). As a result of increased infection, serum cytokines were significantly elevated in CRIg ko mice (Figure S6B). Since bacterial counts in the nonparenchymal (NPC; KC-enriched) and hepatocyte-enriched fractions of the livers of both CRIg wt and ko mice were reduced by greater than 90% during the first 6 hr following infection, increased phagocytosis of bacteria by CRIg wt KCs did not result in increased infection of the liver (Figures 6C and S6D). The reduction in the numbers of bacteria present in the liver cell fractions coincided with a CRIg-independent influx of neutrophils (Figure S6C), confirming the previously described neutrophil-dependence of LM clearance from the liver (Pinto et al., 1991; Conlan and North, 1994; Gregory et al., 2002). In contrast to the liver, bacteria were not efficiently cleared from the spleen of CRIg ko mice early following infection and, as a result, the spleens of CRIg ko mice continued to show increased bacterial counts compared to the spleens of CRIg wt mice (Figures 6C and S6D). In addition, infected spleens in CRIg ko mice showed a 5-fold reduction in splenocyte numbers by day 6 post infection (Figure S6E), demonstrating the functional consequence of inefficient clearance of circulating bacteria in the absence of CRIg. Finally, CRIg ko mice suffered increased mortality compared to wt mice when infected with LM at three different doses (Figure 6D). Thus, through retention of circulating C3-opsonized

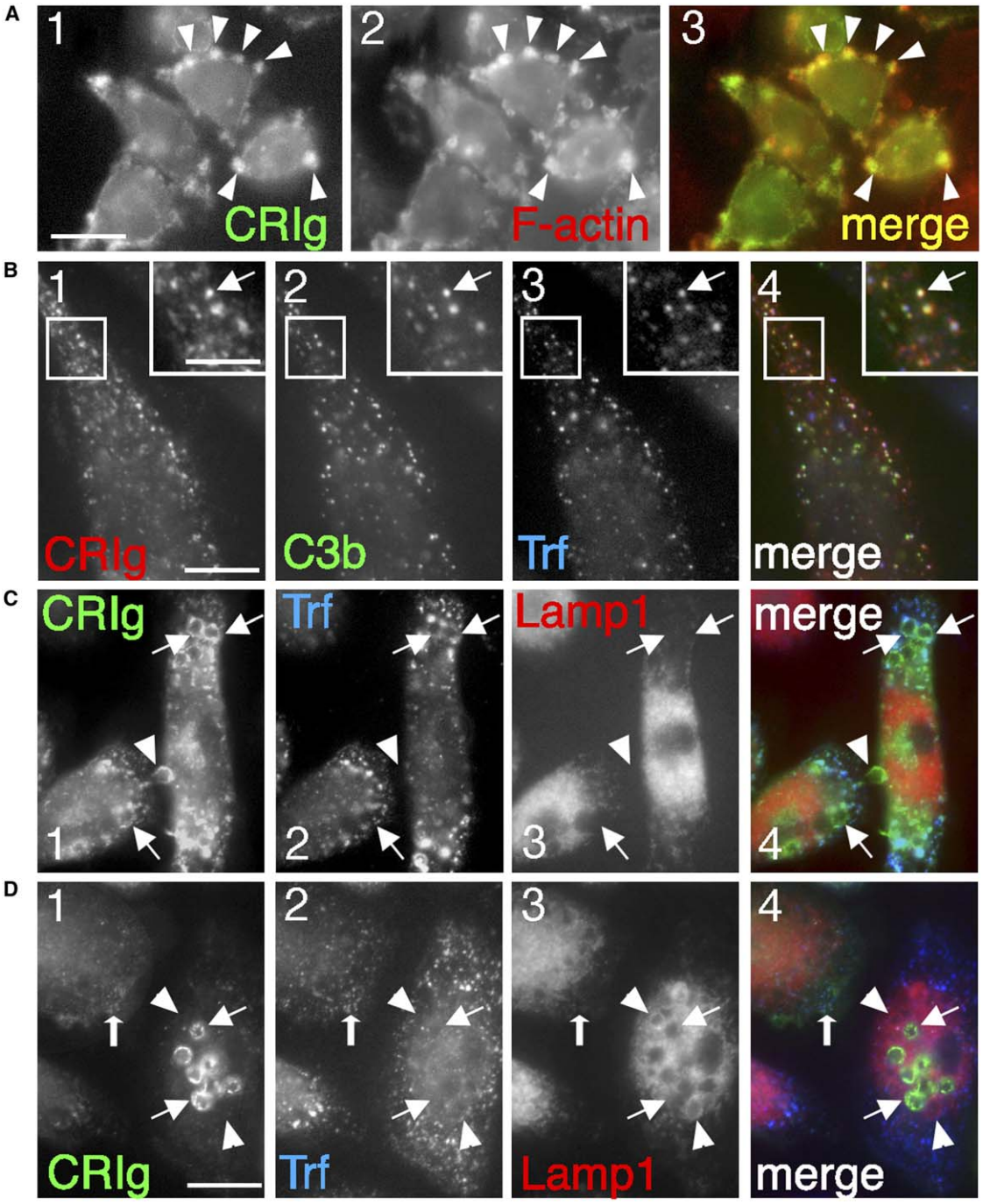

Figure 5. CRIg Is Localized at the Plasma Membrane and on Endosomes that Are Recruited to Sites of Particle Ingestion

(A) Cell surface-expressed CRIg is concentrated at F actin-positive membrane ruffles. Monocyte-derived macrophages cultured for 7–12 days were incubated at 4°C with A488 conjugated anti-CRIg mAb 3C9 (panel 1 and green channel in panel 3), fixed, permeabilized, and counterstained with A546-conjugated phalloidin (panel 2 and red channel in panel 3). Arrowheads indicate membrane ruffles where both CRIg and F-actin staining are more intense than over the rest of the cell surface (yellow in the merged images in panel 3). Scale bar = 20 μm.

(B) CRIg and C3b colocalize with transferrin in endosomes. Macrophages were incubated for 1 hr on ice with anti-CRIg monoclonal antibody (panel 1, red channel in panel 4) or A488-conjugated C3b (panel 2, green channel in panel 4), washed, and then chased for 10 min at 37°C in the presence of A647-conjugated transferrin (panel 3, blue channel in panel 4). Cells were incubated with a secondary Cy3-conjugated donkey anti-mouse Fab'2 antibody following fixation and permeabilization to visualize the anti CRIg antibody. Arrows indicate colocalization of CRIg, C3b, and transferrin in an endosome. Scale bar = 20 μm or 10 μm (insets).

bacteria in the liver, CRIg contributes to efficient clearance of LM from the circulation, preventing infection of other organs and promoting survival of the host.

Since complement opsonization is an important first-line immune defense against *Staphylococcus aureus* (SA) infection (Cunnion et al., 2004), we next determined whether CRIg plays a role in complement dependent phagocytosis of SA, an extracellular bacterium whose natural route of infection is through the circulation. Similar to LM, SA activates the alternative pathway of complement, resulting in deposition of C3b and iC3b on the pathogen surface (Gordon et al., 1988). In C3-sufficient mice, CRIg was required for the efficient hepatic clearance of circulating pathogens. Whereas in CRIg wt mice 91% of the bacteria were recovered in the liver, only 36% of the bacteria were recovered in the liver of CRIg ko mice. The remainder of the inoculum was distributed over blood, spleen, and heart (Figure 7A). In contrast, clearance of circulating bacteria in C3-deficient mice was independent of CRIg status, confirming a role of CRIg as a receptor for C3b and iC3b bound to the pathogens surface. CRIg-dependent binding and uptake of SA by liver KCs were further demonstrated by flow cytometry analysis of hepatic cell fractions (Figure 7B) and immunohistochemistry on liver sections (Figure 7C). Thus, CRIg expression on KCs plays a dominant role in complement C3-dependent removal of both intracellular and extracellular pathogens from the circulation immediately following systemic infection.

DISCUSSION

CRIg Is Required for Capture of C3-Opsonized Pathogens by KCs

Rapid clearance of bacteria from the circulation is a crucial step in the first-line innate immune defense against systemic infection. In this study, we identify a novel complement receptor of the Ig superfamily, CRIg, which is highly expressed on KCs and subsets of other tissue resident macrophages, binds to the C3b and iC3b opsonins, and is required for the rapid removal of pathogens from the circulation. The structure and cellular distribution of CRIg differ from the known complement receptors. CRIg lacks combined C3b and C4b binding short consensus repeat sequences found in CR1 and CR2 as well as the integrin-like domains present in CR3 and CR4. Whereas CR1–CR4 are expressed on a wide variety of cell types, CRIg expression is confined to tissue resident macrophages, including liver KCs.

CRIg's dual binding activity to C3b and iC3b and its abundant expression on liver KCs mediate the efficient capture of intravenously injected LM and SA that are opsonized with both C3 degradation components (Gordon et al., 1988; Croize et al., 1993). Rapid capture of pathogens in the liver is of crucial importance to prevent systemic bacteremia (Hirakata et al., 1991). Once contained by the liver, the pathogens are efficiently eliminated, in part through killing by infiltrating neutrophils (Pinto et al., 1991; Rogers and Unanue, 1993; Conlan and North, 1994; Gregory et al., 1996; Ebe et al., 1999; Gregory et al., 2002). Next to elimination by neutrophils, there may be additional mechanisms by which LM is cleared from the liver. A small portion of the inoculum (~0.1%) was recovered in the gal bladder (results not shown), indicating that some of the LM captured by the liver may be cleared by subsequent biliary excretion in the gastrointestinal lumen (Briones et al., 1992). Inefficient clearance of circulating pathogen leads to an increased LM burden in blood, in turn resulting in increased infection of the spleen where neutrophils are not able to efficiently kill LM (Conlan and North, 1994). The central role of KCs in clearance of circulating pathogens has been shown in studies in which KC depletion results in impaired clearance of LM from the circulation (Pinto et al., 1991; Gregory et al., 2002). Our study now demonstrates that CRIg is the dominant receptor on KCs that mediates complement-dependent clearance of the pathogen from the circulation.

CRIg Recycles on Endosomes

Endosomes play a central role in endocytosis, process elongation, and sorting and delivery of proteins to various subcellular compartments (Steinman et al., 1983). The expression of CRIg on recycling endosomes ensures a readily available supply of CRIg on the cell surface for binding to C3-opsonized particles. CRIg-expressing endosomes are rapidly recruited to sites of particle contact, where they may aid in delivering membrane to the forming phagosome (Aderem and Underhill, 1999; Bajno et al., 2000; Scott et al., 2003; Braun et al., 2004; Stuart and Ezekowitz, 2005).

The subcellular localization and intracellular trafficking of CRIg differ from known complement C3 receptors. Whereas CRIg is localized on constitutively recycling endosomes, CR1, CR3, and CR4 are located on secretory vesicles that fuse with the plasma membrane upon cytokine stimulation of the cells and internalize ligand through a macropinocytotic process only after crosslinking of the receptor (Carpentier et al., 1991). The constitutive

(C) CRIg is recruited to the forming phagosome. Macrophages were incubated with A488-conjugated anti-CRIg antibodies for 20 min at 37°C (panel 1 and green channel in panel 4) then incubated with E-IgM opsonized with C3-sufficient human serum for 10 min at 37°C in the presence of A647-conjugated transferrin (panel 2 and blue channel in panel 4). Cells were stained with A555-conjugated antibodies to Lamp1 post fixation and permeabilization (panel 3 and red channel in panel 4). Arrows indicate localization of CRIg in the forming phagosome; arrowhead indicates the presence of a CRIg-positive phagocytic cup. Scale bar = 20 μm (shown in D).

(D) CRIg is absent in lysosomes. Macrophages were incubated with E-IgM opsonized with C3-sufficient serum for 2 hr at 37°C in the presence of A647-conjugated transferrin (panel 2 and blue channel in panel 4). Following fixation and permeabilization, cells were stained with polyclonal antibodies to CRIg (panel 1 and green channel panel 4) and Lamp1 (panel 3 and red channel in panel 4). Thin arrows show erythrocyes in phagosomes colocalizing with CRIg, but not with transferrin. Arrowheads show erythrocytes in mature phagosomes colocalizing with Lamp1, but not with CRIg. Thick arrows indicate colocalization of CRIg with transferrin and not with erythrocytes. Scale bar = 20 μm.

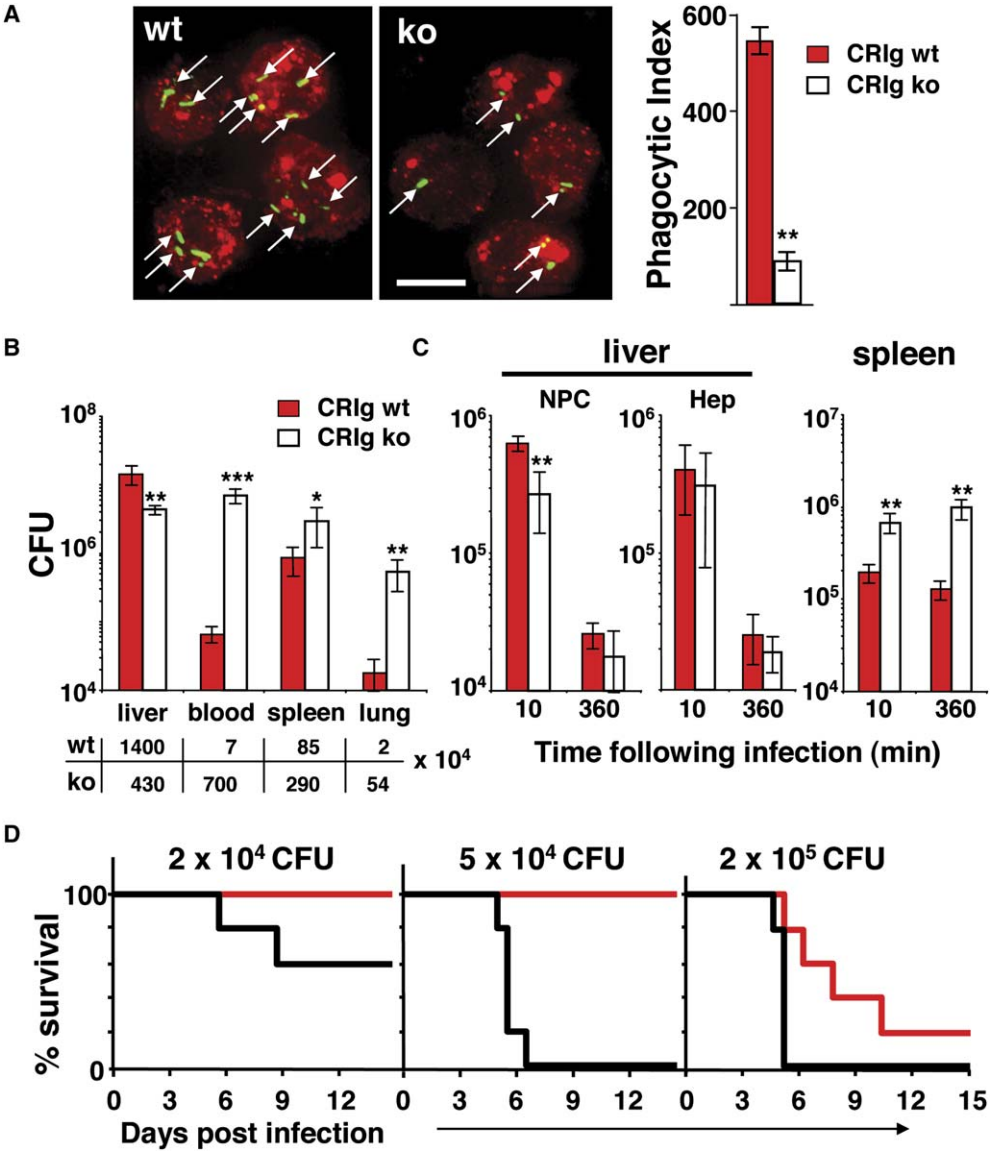

Figure 6. Mice Lacking CRIg Are More Susceptible to *Listeria monocytogenes* Infection

(A) Reduced uptake of *Listeria monocytogenes* (LM)-A488 by CRIg-deficient KCs. Mice were infected with 2×10^7 CFUs live A488-conjugated LM. One hour later, KCs were isolated, incubated with PE-conjugated anti-F4/80, sorted by flow cytometry, and collected on poly-L-lysine-coated slides for observation by confocal microscopy. The number of internalized A488-conjugated LM (arrows, green channel) was counted, and the phagocytic index was calculated. Over 95% of the LM was found inside and not on the surface of the KCs as determined by confocal microscopy. Data represent mean ± SD of four animals per group. Results are representative of three experiments. Statistical analysis (Student's t test): $^{**}p < 0.001$. Scale bar = 10 μm.

(B) Decreased Colony Forming Units (CFUs) in liver and increased bacterial counts in blood, spleen, and lung in CRIg ko mice 10 min following intravenous injection of LM (2×10^7 CFUs). CFUs are expressed per organ or per total pool of peripheral blood. Indicated in a table below the graph are the average numbers of bacteria in each compartment. Data represent mean ± SD of 5–6 animals per group. Statistical analysis (Student's t test): $^{*}p < 0.05$, $^{**}p < 0.005$, $^{***}p < 0.001$.

(C) LM is rapidly cleared from the liver independent of CRIg status. The liver nonparenchymal cell fraction (NPC) and the hepatocyte-enriched fraction (Hep) were separated, and bacterial counts were determined at 10 min and 6 hr following injection of LM (1×10^7 CFU). CFUs are expressed per total cells in the fractions. Over 90% of LM was cleared from the liver during the first 6 hr following infection. Data represent mean ± SD of 4–5 animals per group. Statistical analysis (Student's t test): $^{**}p < 0.005$.

(D) Decreased resistance of CRIg ko mice to LM infection. Survival curves of CRIg wt (red lines) and CRIg ko (black lines) mice infected with the indicated doses of LM following injection into the lateral tail vein; n = 5 per group. Statistical analysis (Wilcoxon): wt versus ko $p < 0.005$ for 2×10^4 and 2×10^5 colony-forming units (CFUs); $p < 0.001$ for 5×10^4 CFUs.

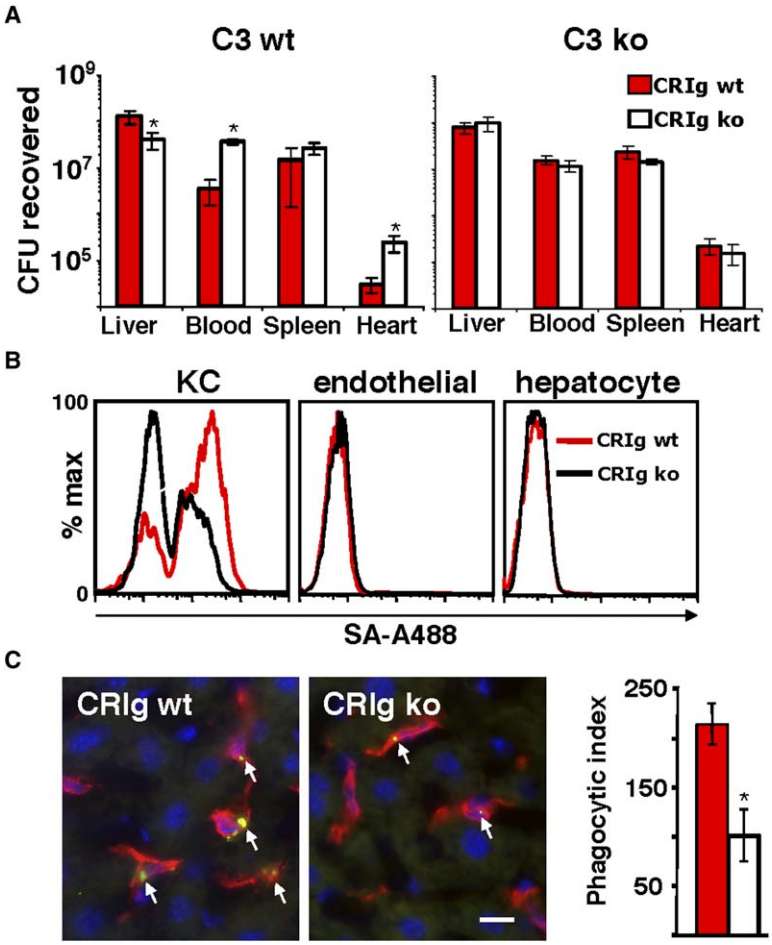

Figure 7. CRIg Is Involved in C3-Dependent Clearance of *Staphylococcus aureus* from the Circulation

(A) Decreased bacterial counts in liver and increased bacterial counts in blood, spleen, and heart in C3-sufficient CRIg ko mice 10 min following intravenous injection with *Staphylococcus aureus* (SA) (5×10^7 CFU). In C3-deficient mice, bacterial counts in the organs or total pool of peripheral blood in CRIg wt and CRIg ko mice are equivalent. Indicated are mean ± SD for 7–10 animals per group. Statistical analysis (Student's t test): *$p < 0.0001$.

(B) Reduced binding of A488-labeled SA to CRIg-deficient KCs. Mice were injected with 2×10^7 CFU live A488-conjugated SA. Liver cells were isolated 1 hour later, incubated with various combinations of antibodies to F4/80, CD45, and CD31, and analyzed by flow cytometry. Kupffer cells were identified as $F4/80^+$ cells, endothelial cells as $CD45^-$ $CD31^+$ cells, and hepatocytes by forward and side scatter. The histograms are representative of three independent experiments.

(C) Fluorescence micrograph showing decreased phagocytosis of SA by Kupffer cells from CRIg ko mice. Mice were infected as described for Figure 7B; liver was fixed 1 hour later; sections were stained with anti-F4/80 and DAPI and visualized by fluorescence microscopy. The number of A488-conjugated SA inside KCs (arrows) were counted, and the phagocytic index was calculated. Data represent mean ± SD of three animals per group. Statistical analysis (Student's t test): *$p < 0.05$. Scale bar = 10 μm.

recycling of CRIg and its endocytosis of ligand in resting macrophages fit with a role in binding of complement-opsonized particles during the initial phase of a bacterial infection prior to generation of an inflammatory response (e.g., the recruitment of activated phagocytes). In addition, CRIg may be involved in the constitutive removal of C3-opsonized apoptotic cells and cell debris, thus preventing local inflammation. How CRIg expression on phagocytes is regulated during an inflammatory response and whether CRIg synergizes with other complement receptors in binding to C3-opsonized particles are areas of future investigation.

In summary, this study identifies a novel macrophage receptor that constitutes an important component of the innate immune system by bridging the central complement component C3 with acute clearance of pathogens. This finding further stresses the critical role of complement and tissue resident macrophages as the first line of immune defense against circulating pathogens.

EXPERIMENTAL PROCEDURES

Cloning and Characterization of Human and Murine CRIg

huCRIg(L) and (S) were cloned from a human fetal library using primers to the Ig folds of A33 antigen. A partial murine CRIg (muCRIg) sequence was assembled from an EST library, and full-length muCRIg was obtained using primers directed to the 3′ and 5′ UTR. Fusion proteins were generated as described in Supplemental Experimental Procedures.

Antibodies and Generation of Stably Transfected Cells

All antibodies were purchased from BD Pharmingen except for anti-F4/80 (Caltag), anti-human CD68 (clone KP-1, Dako), anti-mouse CD68 (clone FA-11, Serotech), and FITC-conjugated polyclonal antibody to mu or huC3 (MP Biomedicals). Cell lines expressing CRIg and monoclonal antibodies to mu and huCRIg were generated as described in Supplemental Experimental Procedures.

Immunohistochemistry

Human liver, collected and snap-frozen at autopsy, was obtained from Ardais Corporation. Liver tissue from 3-month-old CD-1 mice was collected, snap-frozen, and embedded in Optimal Cutting Temperature compound (OCT, Tissue-Tek, Miles Laboratories) at necropsy. For immunohistochemistry, 6 μm cryostat sections obtained from human and mouse liver were incubated with directly conjugated anti-CRIg and anti-CD68 antibodies.

Complement Proteins and Complement-Deficient Serum

Complement C3 was isolated according to the method of Hammer et al. (1991) with an additional protein A column to remove contaminating IgGs. See Supplemental Experimental Procedures for details on the generation of C3 fragments. All other complement proteins and C3- and C5-depleted human serum were purchased from CompTech.

iC3b was purified over a Superdex S-200 10/300 GL gel filtration column to separate monomers from dimers.

Analysis of CRIg Binding to C3 Fragments

C3 or C3 fragments (4 μg/ml) were adsorbed to Maxisorp plates (Nalgene-Nunc) overnight at 4°C. The plate was blocked with PBS, pH 7.4, containing 1% BSA for 2 hr at 22°C, washed 3× with PBS, pH 7.4, containing 0.05% Tween-20 (PBS-T), and incubated with 100 ul serially diluted CRIg proteins for 1 hr at 22°C. Bound CRIg was detected with a 1/3000 dilution of HRPO-conjugated goat anti-human-IgG Ab (Caltag). Detection was visualized with 100 ul TMB (KPL), and the reaction was stopped with 50 ul 2N H_2SO_4. Optical density (O.D.) was measured at 450 nm. All Abs and CRIg proteins were diluted in PBS-T at 100 μl/well. Analysis of the interaction between C3b and CRIg using surface plasmon resonance and flow cytometry analysis of CRIg recycling was performed as described in Supplemental Experimental Procedures.

Immunofluorescence Microscopy and Phagocytosis

Culturing of MDMs, recycling, and phagocytosis assays were performed as described in Supplemental Experimental Procedures.

Animals

All animals were held under Sterile Pathogen Free conditions and housed in a 14 on, 10 hr off light/dark cycle with food and water available ad infinitum. Animal experiments were approved by the Institutional Animal Care and Use Committee of Genentech. CRIg/C3 single- and double-ko mice were generated as described in Supplemental Experimental Procedures.

Microorganisms

Maintenance, inoculation, and phagocytosis of SA (ATCC strain 10832) and LM (ATCC strain 43251) were performed as described in Supplemental Experimental Procedures.

Supplemental Data

Supplemental Data include seven figures, Experimental Procedures, and References and can be found with this article online at http://www.cell.com/cgi/content/full/124/5/915/DC1/.

ACKNOWLEDGMENTS

We would like to acknowledge members of the Immunology Department as well as Drs. Andrew Chan, Flavius Martin, Sherman Fong, Wenjun Ouyang, Alec Cheng, Phil Hass, and Andrew Peden for valuable discussions; Greg Spaniolo for statistical analysis; Zhenyu Gu, Meron Roose-Girma, Michele Bauer, Lucrece Tom, and Willis Su for embryonic stem cell generation; Christine Olsson for advice on genetics; Daniel Tumas and Linda Rangell for pathology support; Tony Liang for the generation and characterization of polyclonal anti-CRIg antibodies; Susan Palmieri for confocal microscopy; Austin Gurney, Yongmei Chen, and Evangeline Abaya for cloning of CRIg; Theresa Shek for generation of anti-CRIg mAbs; Kurt Schroeder for affinity purification of antibodies; Fred Arellano for affinity-purification of CRIg-Fc and –ECD; and Eric Stoelting for graphics support.

Received: June 27, 2005
Revised: September 8, 2005
Accepted: December 9, 2005
Published: March 9, 2006

REFERENCES

Aderem, A., and Underhill, D.M. (1999). Mechanisms of phagocytosis in macrophages. Annu. Rev. Immunol. *17*, 593–623.

Ahn, J.H., Lee, Y., Jeon, C., Lee, S.J., Lee, B.H., Choi, K.D., and Bae, Y.S. (2002). Identification of the genes differentially expressed in human dendritic cell subsets by cDNA subtraction and microarray analysis. Blood *100*, 1742–1754.

Arnaout, M.A., Melamed, J., Tack, B.F., and Colten, H.R. (1981). Characterization of the human complement (c3b) receptor with a fluid phase C3b dimer. J. Immunol. *127*, 1348–1354.

Austin, C.D., De Maziere, A.M., Pisacane, P.I., van Dijk, S.M., Eigenbrot, C., Sliwkowski, M.X., Klumperman, J., and Scheller, R.H. (2004). Endocytosis and sorting of ErbB2 and the site of action of cancer therapeutics trastuzumab and geldanamycin. Mol. Biol. Cell *15*, 5268–5282.

Bajno, L., Peng, X.R., Schreiber, A.D., Moore, H.P., Trimble, W.S., and Grinstein, S. (2000). Focal exocytosis of VAMP3-containing vesicles at sites of phagosome formation. J. Cell Biol. *149*, 697–706.

Benacerraf, B., Sebestyen, M.M., and Schlossman, S. (1959). A quantitative study of the kinetics of blood clearance of P32-labelled Escherichia coli and Staphylococci by the reticuloendothelial system. J. Exp. Med. *110*, 27–48.

Bonifacino, J.S., and Traub, L.M. (2003). Signals for sorting of transmembrane proteins to endosomes and lysosomes. Annu. Rev. Biochem. *72*, 395–447.

Braun, V., Fraisier, V., Raposo, G., Hurbain, I., Sibarita, J.B., Chavrier, P., Galli, T., and Niedergang, F. (2004). TI-VAMP/VAMP7 is required for optimal phagocytosis of opsonised particles in macrophages. EMBO J. *23*, 4166–4176.

Briones, V., Blanco, M.M., Marco, A., Prats, N., Fernandez-Garayzabal, J.F., Suarez, G., Domingo, M., and Dominguez, L. (1992). Biliary excretion as possible origin of Listeria monocytogenes in fecal carriers. Am. J. Vet. Res. *53*, 191–193.

Brown, E.J. (1991). Complement receptors and phagocytosis. Curr. Opin. Immunol. *3*, 76–82.

Carpentier, J.L., Lew, D.P., Paccaud, J.P., Gil, R., Iacopetta, B., Kazatchkine, M., Stendahl, O., and Pozzan, T. (1991). Internalization pathway of C3b receptors in human neutrophils and its transmodulation by chemoattractant receptors stimulation. Cell Regul. *2*, 41–55.

Clark, H.F., Gurney, A.L., Abaya, E., Baker, K., Baldwin, D., Brush, J., Chen, J., Chow, B., Chui, C., Crowley, C., et al. (2003). The secreted protein discovery initiative (SPDI), a large-scale effort to identify novel human secreted and transmembrane proteins: a bioinformatics assessment. Genome Res. *13*, 2265–2270.

Colten, H.R., and Rosen, F.S. (1992). Complement deficiencies. Annu. Rev. Immunol. *10*, 809–834.

Conlan, J.W., and North, R.J. (1994). Neutrophils are essential for early anti-Listeria defense in the liver, but not in the spleen or peritoneal cavity, as revealed by a granulocyte-depleting monoclonal antibody. J. Exp. Med. *179*, 259–268.

Croize, J., Arvieux, J., Berche, P., and Colomb, M.G. (1993). Activation of the human complement alternative pathway by Listeria monocytogenes: evidence for direct binding and proteolysis of the C3 component on bacteria. Infect. Immun. *61*, 5134–5139.

Cunnion, K.M., Benjamin, D.K., Jr., Hester, C.G., and Frank, M.M. (2004). Role of complement receptors 1 and 2 (CD35 and CD21), C3, C4, and C5 in survival by mice of Staphylococcus aureus bacteremia. J. Lab. Clin. Med. *143*, 358–365.

Dussurget, O., Pizarro-Cerda, J., and Cossart, P. (2004). Molecular determinants of Listeria monocytogenes virulence. Annu. Rev. Microbiol. *58*, 587–610.

Ebe, Y., Hasegawa, G., Takatsuka, H., Umezu, H., Mitsuyama, M., Arakawa, M., Mukaida, N., and Naito, M. (1999). The role of Kupffer cells and regulation of neutrophil migration into the liver by macrophage inflammatory protein-2 in primary listeriosis in mice. Pathol. Int. *49*, 519–532.

Fang, Y., Xu, C., Fu, Y.X., Holers, V.M., Zeve, and Molina, H. (1998). Expression of complement receptors 1 and 2 on follicular dendritic cells is necessary for the generation of a strong antigen-specific IgG response. J. Immunol. *160*, 5273–5279.

Fearon, D.T., Kaneko, I., and Thomson, G.G. (1981). Membrane distribution and adsorptive endocytosis by C3b receptors on human polymorphonuclear leukocytes. J. Exp. Med. *153*, 1615–1628.

Gordon, D.L., Rice, J., Finlay-Jones, J.J., McDonald, P.J., and Hostetter, M.K. (1988). Analysis of C3 deposition and degradation on bacterial surfaces after opsonization. J. Infect. Dis. *157*, 697–704.

Gregory, S.H., Sagnimeni, A.J., and Wing, E.J. (1996). Bacteria in the bloodstream are trapped in the liver and killed by immigrating neutrophils. J. Immunol. *157*, 2514–2520.

Gregory, S.H., Cousens, L.P., van Rooijen, N., Dopp, E.A., Carlos, T.M., and Wing, E.J. (2002). Complementary adhesion molecules promote neutrophil-Kupffer cell interaction and the elimination of bacteria taken up by the liver. J. Immunol. *168*, 308–315.

Hammer, C.H., Wirtz, G.H., Renfer, L., Gresham, H.D., and Tack, B.F. (1981). Large scale isolation of functionally active components of the human complement system. J. Biol. Chem. *256*, 3995–4006.

Hirakata, Y., Tomono, K., Tateda, K., Matsumoto, T., Furuya, N., Shimoguchi, K., Kaku, M., and Yamaguchi, K. (1991). Role of bacterial association with Kupffer cells in occurrence of endogenous systemic bacteremia. Infect. Immun. *59*, 289–294.

Holers, V.M., Kinoshita, T., and Molina, H. (1992). The evolution of mouse and human complement C3-binding proteins: divergence of form but conservation of function. Immunol. Today *13*, 231–236.

Hong, K., Kinoshita, T., Pramoonjago, P., Kim, Y.U., Seya, T., and Inoue, K. (1991). Reconstitution of C5 convertase of the alternative complement pathway with isolated C3b dimer and factors B and D. J. Immunol. *146*, 1868–1873.

Jelezarova, E., Luginbuehl, A., and Lutz, H.U. (2003). C3b2-IgG complexes retain dimeric C3 fragments at all levels of inactivation. J. Biol. Chem. *278*, 51806–51812.

Langnaese, K., Colleaux, L., Kloos, D.U., Fontes, M., and Wieacker, P. (2000). Cloning of Z39Ig, a novel gene with immunoglobulin-like domains located on human chromosome X. Biochim. Biophys. Acta *1492*, 522–525.

Metlay, J.P., Witmer-Pack, M.D., Agger, R., Crowley, M.T., Lawless, D., and Steinman, R.M. (1990). The distinct leukocyte integrins of mouse spleen dendritic cells as identified with new hamster monoclonal antibodies. J. Exp. Med. *171*, 1753–1771.

Pangburn, M.K., and Muller-Eberhard, H.J. (1980). Relation of putative thioester bond in C3 to activation of the alternative pathway and the binding of C3b to biological targets of complement. J. Exp. Med. *152*, 1102–1114.

Pinto, A.J., Stewart, D., van Rooijen, N., and Morahan, P.S. (1991). Selective depletion of liver and splenic macrophages using liposomes encapsulating the drug dichloromethylene diphosphonate: effects on antimicrobial resistance. J. Leukoc. Biol. *49*, 579–586.

Portnoy, D.A., Auerbuch, V., and Glomski, I.J. (2002). The cell biology of Listeria monocytogenes infection: the intersection of bacterial pathogenesis and cell-mediated immunity. J. Cell Biol. *158*, 409–414.

Ravetch, J.V., and Bolland, S. (2001). IgG Fc receptors. Annu. Rev. Immunol. *19*, 275–290.

Rogers, H.W., and Unanue, E.R. (1993). Neutrophils are involved in acute, nonspecific resistance to Listeria monocytogenes in mice. Infect. Immun. *61*, 5090–5096.

Scott, C.C., Botelho, R.J., and Grinstein, S. (2003). Phagosome maturation: a few bugs in the system. J. Membr. Biol. *193*, 137–152.

Sengelov, H., Kjeldsen, L., Kroeze, W., Berger, M., and Borregaard, N. (1994). Secretory vesicles are the intracellular reservoir of complement receptor 1 in human neutrophils. J. Immunol. *153*, 804–810.

Smith, D.K., and Xue, H. (1997). Sequence profiles of immunoglobulin and immunoglobulin-like domains. J. Mol. Biol. *274*, 530–545.

Steinman, R.M., Mellman, I.S., Muller, W.A., and Cohn, Z.A. (1983). Endocytosis and the recycling of plasma membrane. J. Cell Biol. *96*, 1–27.

Stuart, L.M., and Ezekowitz, R.A. (2005). Phagocytosis: elegant complexity. Immunity *22*, 539–550.

Underhill, D.M., and Ozinsky, A. (2002). Phagocytosis of microbes: complexity in action. Annu. Rev. Immunol. *20*, 825–852.

Vazquez-Boland, J.A., Kuhn, M., Berche, P., Chakraborty, T., Dominguez-Bernal, G., Goebel, W., Gonzalez-Zorn, B., Wehland, J., and Kreft, J. (2001). Listeria pathogenesis and molecular virulence determinants. Clin. Microbiol. Rev. *14*, 584–640.

Walker, M.G. (2002). Z39Ig is co-expressed with activated macrophage genes. Biochim. Biophys. Acta *1574*, 387–390.

Walport, M.J. (2001a). Complement. First of two parts. N. Engl. J. Med. *344*, 1058–1066.

Walport, M.J. (2001b). Complement. Second of two parts. N. Engl. J. Med. *344*, 1140–1144.

Wu, H., Prince, J.E., Brayton, C.F., Shah, C., Zeve, D., Gregory, S.H., Smith, C.W., and Ballantyne, C.M. (2003). Host resistance of CD18 knockout mice against systemic infection with Listeria monocytogenes. Infect. Immun. *71*, 5986–5993.